State-space framework for estimating measurement error from double-tagging telemetry experiments

Article *in* Methods in Ecology and Evolution · January 2011

7 authors, including:

Ian D Jonsen
Macquarie University
87 PUBLICATIONS **2,307** CITATIONS

SEE PROFILE

Patrick Robinson
University of California, Santa Cruz
59 PUBLICATIONS **946** CITATIONS

SEE PROFILE

Daniel P Costa
University of California, Santa Cruz
527 PUBLICATIONS **13,969** CITATIONS

SEE PROFILE

Barbara A Block
Stanford University
292 PUBLICATIONS **10,651** CITATIONS

SEE PROFILE

Some of the authors of this publication are also working on these related projects:

Bayesian State-space models for Animal Movement (bsam) View project

Resolving the warming East Australian Current's impact on a marine food web View project

State-space framework for estimating measurement error from double-tagging telemetry experiments

Arliss J. Winship[1]*†, Salvador J. Jorgensen[2], Scott A. Shaffer[3], Ian D. Jonsen[1], Patrick W. Robinson[4], Daniel P. Costa[4] and Barbara A. Block[2]

[1]*Department of Biology, Dalhousie University, Halifax, NS B3H 4J1, Canada;* [2]*Department of Biology, Stanford University, Pacific Grove, CA 93950, USA;* [3]*Department of Biological Sciences, San José State University, San José, CA 95192, USA;* and [4]*Department of Ecology and Evolutionary Biology, University of California Santa Cruz, Santa Cruz, CA 95064, USA*

Summary

1. Double-tagging experiments are invaluable for determining the accuracy and precision of location data provided by different telemetry technologies used with free-ranging animals.

2. We developed a state-space modelling framework for estimating the precision of telemetry location data based on double-tagging experiments. The model is simultaneously fitted to multiple data types with different temporal resolutions while including errors in all data.

3. We used the model to estimate the precision of a specific geolocation method based on light and sea surface temperature applied to a large marine telemetry dataset. Data were available from double-tagging experiments on 111 animals representing seven marine species including 4 sharks, 2 birds and 1 pinniped. Study animals carried electronic tags that provided geolocation estimates as well as more precise satellite-based location data (Argos and Global Positioning System).

4. Estimates of the precision of geolocations were similar to previous findings. The overall estimated SD of geolocation errors for each species ranged from 0·5 to 3·9° for longitude and 0·8 to 3·6° for latitude.

5. While these results are specific to this particular type of location estimation method, the state-space framework presented here is a robust approach to estimating the precision of various types of telemetry location data from double-tagging experiments. The model simultaneously allows for appropriate inferences about true animal locations and movement.

Key-words: Argos, birds, electronic tagging, geolocation, Global Positioning System, pinnipeds, precision, sharks

Introduction

A variety of methods and technologies are used to remotely track the movements of wild animals. The marine environment poses particular challenges to tracking as animals range widely in the open sea and are often far from land. Furthermore, many marine fish and mammals spend most of their time submerged. Nevertheless, researchers have had great success tracking marine animals using electronic devices, or tags, that are attached to the animals (Kooyman 2004; Hooker *et al.* 2007). For animals that spend all or part of their time at the surface, technologies that use satellite systems such the Argos system and the Global Positioning System (GPS) can provide

relatively precise estimates of an animal's geographic location when the tag's antenna is out of the water (McConnell *et al.* 1992; Weimerskirch *et al.* 2002; Weng *et al.* 2005). These technologies are problematic for animals that spend prolonged periods of time underwater because of their reliance on radio transmission through air and real-time communication with satellites. Geolocation methods use a variety of algorithms to estimate the geographic location of an animal from archived data such as time, light, depth and water temperature, and these methods have been used to estimate the movement paths of many animals (DeLong *et al.* 1992; Metcalfe & Arnold 1997; Block *et al.* 2001; Shaffer *et al.* 2006). Light-based geolocation methods rely on archived data on solar irradiance, which can be used to determine the time of sunrise and sunset. The timing of sunrise and sunset provides information on the time of midday and day length, which can be used to estimate longitude and latitude (Smith & Goodman 1986; Hill 1994; Ekstrom 2004). Light-based geolocations are usually less

*Correspondence author. E-mail: awinship@ucsc.edu
Correspondence site: http://www.respond2articles.com/MEE/
†Current address: University of California, Santa Cruz, CA, USA.

precise than location estimates derived from satellite-based technologies. For example, day length is informative about latitude near the solstices, but much less so near the equinoxes (Ekstrom 2007; Sibert *et al.* 2009). The precision of light-based latitude geolocations can be improved using archived data on other environmental variables such as depth and sea surface temperature (SST; Beck *et al.* 2002; Teo *et al.* 2004; Nielsen *et al.* 2006). Nevertheless, geolocations tend to vary in their precision and are limited to estimates that occur once or twice a day because of the integration of data across several hours or more to estimate the time of sunrise and sunset and SST.

Quantifying the uncertainty in location estimates is vital for drawing proper biological inferences from tracking data. Location estimates from any technology should be validated to assess their accuracy and precision. Validation requires knowledge of the true location of the tag. Many studies have assessed the accuracy and precision of Argos and geolocation estimates using tags placed at known locations (e.g. Musyl *et al.* 2001; Nicholls *et al.* 2007). Other studies have attempted to replicate more realistic conditions by validating location estimates from tags attached to captive animals at known locations (Vincent *et al.* 2002; Schaefer & Fuller 2006) or by use of endpoint data (Teo *et al.* 2004). Only free-ranging animals can provide a true test of a technology under realistic behavioural and environmental conditions, but then one must rely on some tracking technology to determine their true location. The approach that researchers have commonly taken to validate tracking technology on wild animals is double tagging. In double-tagging experiments, two tracking technologies are used simultaneously on the same animal; one technology that provides location estimates with relatively high precision and another technology that provides estimates that require validation and are assumed to be less precise. Technology pairings have included GPS and Argos (Kuhn *et al.* 2009; Costa *et al.* 2010; Patterson *et al.* 2010), GPS and geolocation (Tremblay *et al.* 2009) and Argos and geolocation (Phillips *et al.* 2004; Teo *et al.* 2004). Often the accuracy and precision of the latter estimates have been assessed by assuming that the former estimates represent the true locations. The difficulty with this assumption is that no technology currently provides location estimates without error, although some estimates can be very accurate and precise (e.g. GPS). Furthermore, direct comparison of two location data sets is often complicated by differences in timing whereby data pairs do not correspond exactly in time.

Animal movement is often modelled as a partially random process (Codling *et al.* 2008). To make inferences about animal movement from imperfect estimates of animal locations requires a statistical framework that accounts for stochasticity in the underlying modelled process and errors in the observations of the true state of the system. State-space models provide such a statistical framework and are useful for analysing dynamic processes such as population dynamics and movement from time-series data (Durbin & Koopman 2001; Buckland *et al.* 2004; Patterson *et al.* 2008). State-space models of animal movement have been developed and fitted to GPS (Morales *et al.* 2004), Argos (Jonsen *et al.* 2005), geolocation (Sibert *et al.* 2003) and light data (Nielsen & Sibert 2007).

Observation error in these models has been treated in a variety of ways including the assumption of no observation error (Morales *et al.* 2004), fixed observation error determined from a separate analysis (Jonsen *et al.* 2005) and estimation of observation error within the state-space framework itself (Sibert *et al.* 2003). A state-space model is an ideal statistical tool for validating location estimates from double-tagging experiments because it can be fitted to multiple data sets simultaneously while accounting for observation errors arising from both technologies. Furthermore, data from different data sets do not need to correspond in time because the data relate only to the common underlying estimated states or locations, not to each other.

The primary objective of our study was to develop and demonstrate a state-space modelling framework for estimating the precision of location data from double-tagging experiments. We applied the framework to data from a number of double-tagging experiments conducted on seven marine species from a range of taxa including birds, sharks, and pinnipeds. For each species, two types of location data were available: satellite-based estimates (Argos or GPS) and geolocations. We used the model to estimate the precision of geolocations while accounting for errors in the satellite-based estimates. Thus, a secondary objective of our study was to provide quantitative estimates of the uncertainty inherent to a common type of geolocation data available for marine animals. Our modelling framework is general and flexible and can be adapted to any situation with multiple location data sets to estimate the precision of those data and make inferences about the animal's true underlying locations and movement.

Materials and methods

DATA

We analysed data from double-tagging experiments on seven marine species (Table 1): blue shark (*Prionace glauca* Linnaeus, 1758), Galápagos shark (*Carcharhinus galapagensis* Snodgrass and Heller, 1905), short-finned mako shark (*Isurus oxyrinchus* Rafinesque, 1810), salmon shark (*Lamna ditropis* Hubbs and Follett, 1947), black-footed albatross (*Phoebastria nigripes* Audubon, 1839), Laysan albatross (*P. immutabilis* Rothschild, 1893) and California sea lion (*Zalophus californianus* Lesson, 1828). For each species, two types of location data were available: satellite-based estimates (Argos or GPS) and geolocations. The geolocations we analysed were longitudes derived using light-based methods (Lotek onboard algorithms and WC-GPE software version 1.2.5 Wildlife Computers 2005) and latitudes derived using the algorithm described in Teo *et al.* (2004). Briefly, the latitude algorithm used the longitude geolocations and data on SST to sequentially estimate the latitudes that resulted in the best correspondence between SST measured by the tag and independent, remotely-sensed estimates of SST. Remotely-sensed SST data with a spatial resolution of 4 km were used preferentially but coarser grids (9 km) were used when cloud cover resulted in difficulties for the geolocation algorithm. The temporal resolution of the SST data was daily (night-time).

There were extended periods of time without Argos/GPS data in some tracks because of prolonged submergence, hauling out on land (sea lions) or tag failure. To avoid the model fitting the geolocation

Table 1. Number of individuals, track lengths and numbers of data (Argos/Global Positioning System (GPS) and geolocation) by species. All values except *n* are medians across individuals with ranges in parentheses. Track length represents the number of days with Argos/GPS data

Species	*n*	Track length (d)	Argos/GPS	Geolocation
Sharks				
Blue	14	97 (23–301)	129 (28–504)	11 (5–26)
Galápagos	2	33 (22–43)	58 (54–62)	9 (6–11)
Mako	25	255 (47–706)	490 (109–1217)	21 (7–97)
Salmon	34	512 (18–1311)	653 (46–1336)	19 (5–85)
Birds				
Black-footed albatross	12	11 (10–22)	265 (165–405)	10 (5–15)
Laysan albatross	15	19 (9–32)	437 (192–693)	16 (6–24)
Pinnipeds				
California sea lion	9	79 (74–86)	953 (727–1749)	55 (30–64)

data too closely during these data gaps and thereby underestimating geolocation errors, we only analysed geolocations from GMT dates with Argos/GPS data. Also, geolocations based on poor-quality light data were manually selected and excluded from our analysis. There were few geolocations for some animals as a result of tag failure and poor-quality light data, especially on shorter tracks (e.g. birds). Therefore, we limited our analysis to animals with ≥5 geolocations. Two sharks with the lowest frequencies of Argos data were excluded from our analysis as we were unable to obtain good estimates of their geolocation errors.

Details about the tagging methods (technologies, dates and locations) are described in the Supporting Information ('Tagging methods' section in Data S1).

MODEL

We used a state-space framework to model stochastic animal movement while admitting errors in the 'observation' of an animal's location. The model was fitted to data from each individual animal separately and was fitted simultaneously to both data sets for each animal, the relatively precise set of location data (Argos or GPS) and the geolocation data. A Bayesian statistical framework was used to estimate probability distributions for the states (animal locations), movement parameters and the precisions of the observation errors for the geolocation data.

Secondarily, we were interested in how well a model fitted only to the geolocation data for an individual animal would perform in terms of capturing the estimated locations from the model that was also fitted to the Argos/GPS data for that individual. We assumed that the latter model provided a more accurate estimate of an animal's path, and we were interested in how similar the estimated path would have been if only the geolocation data had been available, which is the case in most geolocation tagging studies. Fitting the model only to the geolocation data for an individual required estimates of the geoloca-

tion error. We took a leave-one-out approach to avoid transfer of information between the two models for an individual. For each individual, we calculated a group-specific geolocation error using all animals of the same group (sharks, birds or pinnipeds) excluding that individual. The state-space model was then fitted only to the geolocation data for that animal with the geolocation error fixed at these group-specific point estimates, which were not informed by that individual's data. We then compared the regular, estimated locations corresponding exactly in time between the geolocation-only and Argos/GPS-and-geolocation model for each individual. Specifically, we calculated the proportion of mean location estimates from the latter model that fell within the 95% intervals of posterior probability for the corresponding location estimates from the former model. This analysis allowed us to evaluate whether group-specific point estimates of geolocation errors were suitable for fitting the model to a novel individual track with only geolocation data. Comparisons of estimated locations between the geolocation-only model and the Argos/GPS-and-geolocation model for each individual were restricted to locations with both types of data within ± 1 day to avoid comparing unrealistic location estimates during extended data gaps. Interpolation error increases with the length of a data gap but this error should have been small within ± 1 day (Lonergan *et al.* 2009).

All analyses were performed using the free software R (R Development Core Team 2009) and WinBUGS (Lunn *et al.* 2000). The WinBUGS code for the Argos/GPS-and-geolocation model is presented in the Supporting Information ('WinBUGS code' section in Data S1). Wide, flat prior probability distributions were assumed for the model parameters (Table 2). Two thousand samples from the joint posterior probability distribution were obtained by running two chains each of length 500 000, discarding the initial 100 000 samples, and keeping every 400th of the remaining samples. We checked convergence of the error parameter estimates using the potential scale reduction factor, $\hat{R}$; values close to 1 were consistent with convergence (Gelman & Rubin 1992). $\hat{R}$ was < 1.01 for all error parameter estimates, and

Table 2. Prior probability distributions assumed for model parameters and states. The *t*-distribution was used for the $x_{\text{lon},1}$ and $x_{\text{lat},1}$ priors when fitting the model to Argos/Global Positioning System (GPS) and geolocation data (1) and the normal distribution was used when fitting the model only to geolocation data (2). In both cases, $y_{\text{lon},1}$ and $y_{\text{lat},1}$ represent the known deployment location

Estimated quantity	Description	Prior
γ	movement correlation	Beta($\alpha = 1, \beta = 1$)
θ	turning angle	U($a = -\pi, b = \pi$)
$\boldsymbol{\Sigma}$	movement variance	Inv-Wishart ($S^{-1} = \mathbf{I}, v = 2$)
$x_{\text{lon},1}$	initial longitude (1)	$t(\mu = y_{\text{lon},1}, \sigma^2 = 0.01, v = 2)$
$x_{\text{lon},1}$	initial longitude (2)	N($\mu = y_{\text{lon},1}, \sigma^2 = 1e{-}8$)
$x_{\text{lat},1}$	initial latitude (1)	$t(\mu = y_{\text{lat},1}, \sigma^2 = 0{\cdot}01, v = 2)$
$x_{\text{lat},1}$	initial latitude (2)	N($\mu = y_{\text{lat},1}, \sigma^2 = 1e{-}8$)
$\log \psi$	Argos/GPS error scale	U($a = -10, b = 10$)
$\log \tau_{\text{lon}}, \log \tau_{\text{lat}}$	precision of geolocation data	U($a = -1000, b = 1000$)

comparisons of estimated locations between Argos/GPS-and-geolocation and geolocation-only models were limited to locations with $\hat{R} < 1.1$ in both models.

PROCESS MODEL

The process model describing animal movement was the first-difference correlated random walk model described by Jonsen *et al.* (2005). The basic movement equation was:

$$\mathbf{x}_{t+1} = \mathbf{x}_t + \mathbf{d}_t \qquad \text{eqn 1}$$

where $\mathbf{x}_t$ is a vector of length 2 representing the true longitude and latitude of the animal (in degrees) at time t and $\mathbf{d}_t$ is a vector representing the movement in longitude and latitude between times t and $t+1$. Movements are correlated over time such that

$$\mathbf{d}_t = \gamma \mathbf{T} \mathbf{d}_{t-1} + \boldsymbol{\eta}_t \qquad \text{eqn 2}$$

where γ is a parameter specifying the correlation between subsequent movements, $\mathbf{T}$ is a transition matrix specifying the mean direction of movement and $\boldsymbol{\eta}_t$ is the stochastic deviation in movement between times t and $t+1$. The movement transition matrix, $\mathbf{T}$, is parameterized by the mean turning angle, θ:

$$\mathbf{T} = \begin{bmatrix} \cos\theta & -\sin\theta \\ \sin\theta & \cos\theta \end{bmatrix} \qquad \text{eqn 3}$$

Stochastic deviations in movement, $\boldsymbol{\eta}_t$, were assumed to be normally distributed with mean 0 and variance–covariance matrix, $\boldsymbol{\Sigma}$:

$$\boldsymbol{\Sigma} = \begin{bmatrix} \sigma_{\text{lon}}^2 & \rho\sigma_{\text{lon}}\sigma_{\text{lat}} \\ \rho\sigma_{\text{lon}}\sigma_{\text{lat}} & \sigma_{\text{lat}}^2 \end{bmatrix} \qquad \text{eqn 4}$$

where σ_{lon}^2 and σ_{lat}^2 are the variances of longitudinal and latitudinal movement deviations, respectively, and ρ is the correlation coefficient.

The estimated quantities in the process model were the true locations (states) at each point in time, $\mathbf{x}_t$ and the movement parameters γ, θ and $\boldsymbol{\Sigma}$. Speed was not an estimated parameter but rather the resultant vector specified by $\mathbf{d}_t$ for a given time step. As a result, there was no explicit prior probability distribution for speed. The implicit prior for speed during a given time step was a function of the speed during the previous time step and the movement parameters.

Our model assumed linear movement within a time step. We used a time step of 6 h for albatrosses and sea lions and 1 day for sharks. We chose a shorter time step for birds and sea lions because the average number of Argos/GPS data per day was higher (Table 1). Furthermore, the shorter time step allowed for a more realistic description of the movement of birds and sea lions, especially given the relatively high travel speed of birds and the periodic haul-out behaviour of sea lions. A 1-day time step was used for all species when fitting the geolocation-only model because the geolocation data were less frequent.

OBSERVATION MODEL

The observation model related the three types of data, Argos, GPS and geolocation, to the true animal locations:

$$\mathbf{y}_i = \boldsymbol{\mu}_i + \boldsymbol{\epsilon}_i \qquad \text{eqn 5}$$

where $\mathbf{y}_i$ is the ith $(i = 1,2,\ldots n)$ pair of longitude and latitude data, $\boldsymbol{\mu}_i$ is the corresponding true longitude and latitude and $\boldsymbol{\epsilon}_i$ are random, serially independent observation errors. True locations, $\boldsymbol{\mu}_i$, were calculated from the estimated states that were regular in time, $\mathbf{x}_t$, according to

$$\boldsymbol{\mu}_i = (1 - j_i)\mathbf{x}_t + j_i\mathbf{x}_{t+1} \quad \text{for} \quad i \in I_t \qquad \text{eqn 6}$$

where I_t is the set of observations that occurs between times t and $t + 1$ and the scalar $j_i(0 < j_i < 1)$ is the proportion of this time step that elapsed prior to $\boldsymbol{\mu}_i$.

A scaled *t*-distribution was assumed for errors in Argos data following Jonsen *et al.* (2005) so that $\epsilon_{i,\text{lon}} \sim t\left(0, \psi\tau_{\text{lon},q_i}, v_{\text{lon},q_i}\right)$ and similarly for latitude, where q_i is the Argos location quality class of $\mathbf{y}_i$, $\tau_{\text{lon},q}$ and $v_{\text{lon},q}$ are the precision scale parameter and degrees of freedom of the *t*-distribution, respectively, for location quality class q and ψ is an estimated parameter that allows the scale of errors to vary because of variability among tags. The values of $\tau_{\text{lon},q}$, $\tau_{\text{lat},q}$, $v_{\text{lon},q}$ and $v_{\text{lat},q}$ for each of the six Argos location quality classes (3, 2, 1, 0, A, B) were fixed at the values derived by Jonsen *et al.* (2005) from their analysis of Argos data from seals in captivity at a known location (Vincent *et al.* 2002). Location quality class Z occurred in the bird data and was assumed to be of the same quality as class B, although estimates of quality Z are often much less precise.

For lack of better information, errors in GPS data were assumed to follow the same distribution as Argos errors for the best location quality class, 3. It is important to note that the precision and distribution of errors in GPS data almost surely differ from those of even high-quality Argos data. For example, the GPS data might have been more precise than we assumed. Nevertheless, given the relatively high precision of Argos location quality class 3 and the low precision of the geolocation data, higher-precision GPS data would have had very little effect on our estimates of the precision of the geolocation data.

As noted earlier, the geolocation 'data' are themselves a complex function of light and SST data. In the absence of a more appropriate error model for these geolocation data, we used the normal distribution as an approximation where $\epsilon_{i,\text{lon}} \sim N(0, \tau_{\text{lon}})$ and similarly for latitude. The geolocation data did not exhibit extreme outliers as did the Argos data, so the normal distribution was more appropriate than the t distribution. The precisions of geolocation errors, τ_{lon} and τ_{lat}, were the estimated parameters of primary interest. We subsequently report these geolocation error estimates as standard deviations, SD_{lon} and SD_{lat}. We assumed uninformative log-uniform priors for the precisions of the geolocation data (Table 2; Gelman *et al.* 2004).

Estimated locations were essentially fixed at known deployment and recovery locations. For the Argos/GPS-and-geolocation model, deployment and recovery location data were assumed to be *t*-distributed with a very high precision (error SD of 10 m) and degrees of freedom (100 000). For the geolocation-only model, deployment and recovery location data were assumed to follow a normal distribution with the same precision as in the Argos/GPS-and-geolocation model.

Estimates of longitude and latitude geolocation errors were calculated for each individual animal, species and species group (sharks, birds and pinnipeds). Details about how these estimates were calculated from the posterior probability distributions are described in the Supporting Information ('Error estimates' section in Data S1).

Results

The mean estimated travel paths of the animals more closely matched the satellite-based data (Argos/GPS) than the geolocation data when the state-space model was simultaneously fitted to both data (Fig. 1, Figs S1–S7). The satellite-based data were more precise, thus the model fitted these data more closely. The mean estimated travel paths of the animals were plausible except during extended gaps in the Argos/GPS data. For example, no GPS data were available during periods when
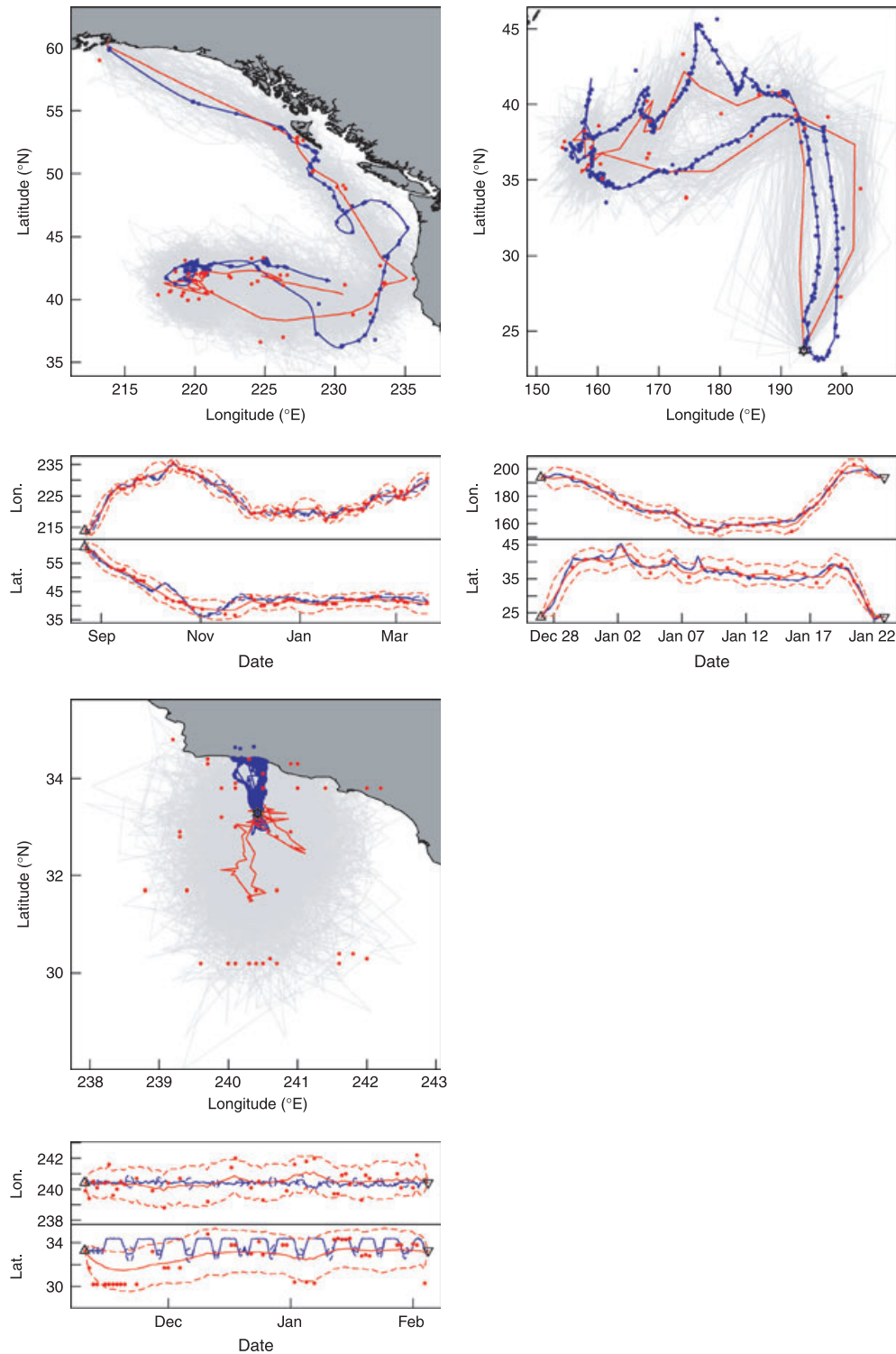
Fig. 1. State-space model fitted to Argos/Global Positioning System (GPS) and geolocation data for three example individuals (a–c, salmon shark #16; d–f, Laysan albatross #6; g–i, California sea lion #9). Blue and red points represent Argos/GPS and geolocation data, respectively. Blue and red lines represent the mean estimated paths from the state-space model fitted to Argos/GPS and geolocation data simultaneously and only geolocation data, respectively. Dashed lines represent intervals of 95% posterior probability. Light grey lines in panels a, d and g represent a sample of estimated paths ($n = 100$) from the posterior probability distribution of the geolocation-only model. Triangles indicate known deployment and inverted triangles indicate known recapture locations. Dark grey represents land. Note that some outlying Argos data are outside of the plot boundaries and are not shown.

sea lions were hauled out on land. Thus, the model was unconstrained during haul-out periods, which resulted in mean estimated locations that were often slightly different from the location of the haul-out and large uncertainties in these mean location estimates (Fig. 1, Fig. S7). Posterior probability intervals for estimated locations were relatively narrow when the model was fitted to Argos/GPS and geolocation data, except during data gaps.

The residual differences between the geolocation data and the estimated paths were often quite large (several degrees or more) and were variable among individuals and species (Fig. 2). Longitude residuals were generally centred around zero. Latitude residuals were also generally centred around zero, but a substantial negative bias was evident in the latitude geolocations for many salmon sharks and sea lions. The bias in latitude geolocations for salmon sharks was greater at higher
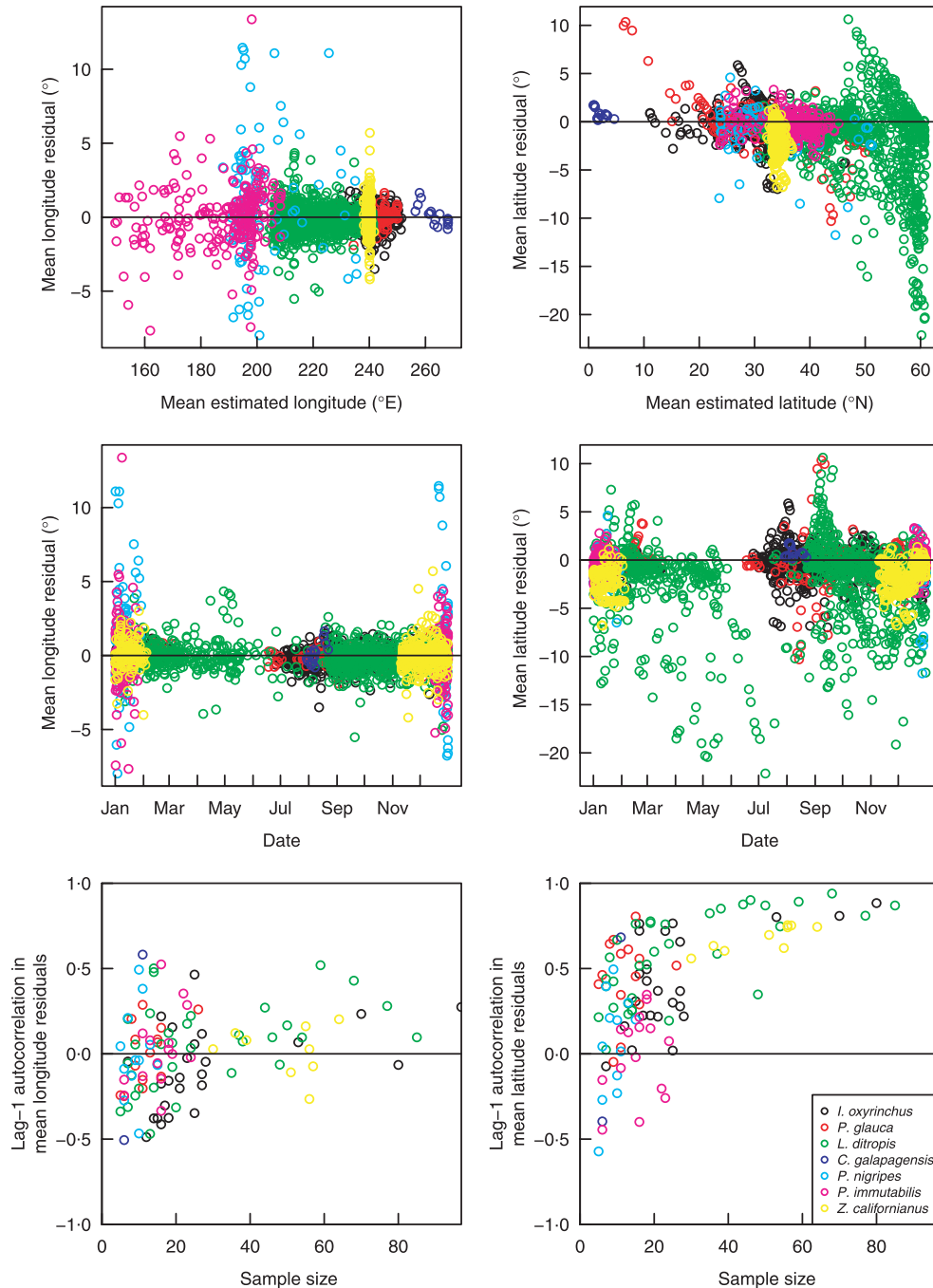
Fig. 2. Geolocation residuals from the model fitted to Argos/Global Positioning System and geolocation data. The top panels show all longitude and latitude residuals (posterior mean residuals) plotted by the corresponding mean estimated longitudes and latitudes for all individuals. The middle panels show these residuals plotted by day of the year for all individuals. The bottom panels show the lag-1 autocorrelation in these residuals for each individual plotted by sample size (the number of residuals or geolocation data per individual). Note that the time between successive geolocation data was not constant so the autocorrelation does not correspond to a fixed time interval.

latitudes with a mean bias of −3·2° at estimated latitudes > 50°N, but only −0·9° at latitudes < 50°N. There were no obvious trends in residual errors with time of year, aside from the confounding of interspecific differences with date (Fig. 2). There was no strong evidence of a general sequential autocorrelation in longitude residuals, but latitude residuals were positively autocorrelated over time (Fig. 2). The autocorrelation in latitude residuals was increasingly evident as the length of tracks (i.e. sample size) increased (Fig. 2). There was little evidence of a strong correlation between longitude and latitude residuals; Pearson's correlation coefficient, r, was 0·02 ($P > 0·4$) and 0.06 ($P < 0·01$) for the residuals and absolute residuals, respectively. Less than 15% of individuals had significant correlations between longitude and latitude residuals ($\alpha = 0·05$); these individuals were spread relatively evenly among species, and the significant correlations were positive and negative. These findings suggest that there was no clear correlative pattern between longitude and latitude geolocation errors. There was a significant positive correlation between absolute longitude geolocation residuals and estimated latitude for salmon sharks but not for any other species. However, this correlation was not significant when estimated latitudes > 55°N were excluded.

The posterior probability distributions for the estimated geolocation errors were unimodal, well-defined and differed from the assumed prior probability distribution (Figs S8–S15). The estimated errors in geolocations varied among individuals and species and between longitude and latitude (Table 3, Table S1, Fig. 3). Estimated longitude error SDs were < 1° for sea lions and all four shark species, while the estimated longitude errors for birds were one or more degrees greater. The birds also exhibited the widest range in longitude errors among individuals. Estimated latitude errors were greater than longitude errors for all species except birds. Estimated latitude errors were < 2° for three of the shark species and both birds. Sea lions had a slightly greater estimated latitude error (2·2 ± 0·08°), and salmon sharks had the highest, most variable estimated latitude errors (3·6 ± 0·08°).

The mean estimated locations from the geolocation-only model differed from the mean estimated locations from the Argos/GPS-and-geolocation model (Fig. 1, Supplementary Figs S1–S7). The mean estimated paths were generally plausible except during gaps in the geolocation data. The estimated paths of the sea lions failed to capture the periodic trips to the
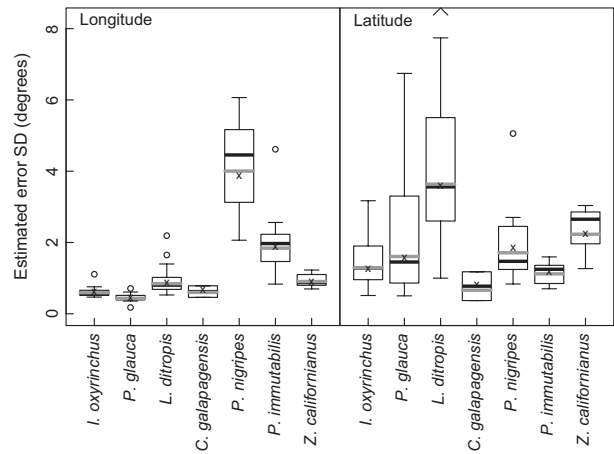

Fig. 3. Estimated SD of errors in longitude and latitude geolocations by species. Each boxplot represents the distribution of SDs among individuals with the thick black line indicating the median, the grey line indicating the mean and the *x* indicating the weighted mean. Note the latter two were calculated on the log-scale then back-transformed. The arrow at the top of the latitude panel indicates an outlying individual *L. ditropis* value, 18·0, that is not shown.

haul-out because the geolocation data were less frequent and less precise. The lower frequency and precision of the geolocation data also provided less constraint on estimated movements resulting in many implausible paths in the sample of paths from the posterior probability distribution (e.g. movements over land, large rapid movements; Fig. 1, Supplementary Figs S1–S7). The posterior probability intervals for the estimated locations were much wider for the geolocation-only model (Fig. 1). The proportion of mean estimated longitudes and latitudes from the Argos/GPS-and-geolocation model that fell within the 95% posterior probability interval for the corresponding estimates from the geolocation-only model varied among individuals and species (Fig. 4, Supplementary Table S1). Coverage was better for longitude with 69% of individuals having ≥95% of their mean longitudes from the former model within the 95% intervals from the latter model. With respect to latitude, only 38% of individuals had ≥95% coverage. Mako and blue sharks had the highest percentages of individuals with ≥95% coverage of longitude (96% and 100%, respectively), followed by sea lions and Laysan albatrosses (67%). About 56% and 50% of salmon sharks and Galápagos sharks had ≥95% longitude coverage, respectively,

Table 3. Estimated SD of errors in longitude ($\widehat{SD}_{lon}$) and latitude ($\widehat{SD}_{lat}$) geolocations (degrees) by group and species. The SDs of these estimates are also presented ($\sigma_{\widehat{SD}_{lon}}$ and $\sigma_{\widehat{SD}_{lat}}$)

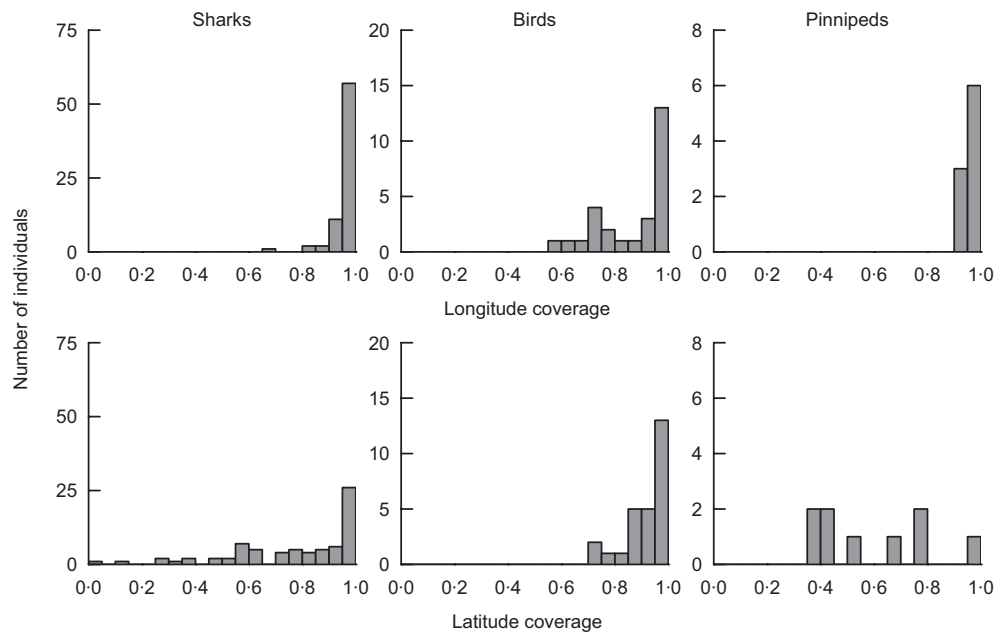| Species	$\widehat{SD}_{lon}$	$\sigma_{\widehat{SD}_{lon}}$	$\widehat{SD}_{lat}$	$\sigma_{\widehat{SD}_{lat}}$
Sharks	0·7	0·01	2·2	0·04
Blue	0·5	0·03	1·6	0·09
Galápagos	0·7	0·12	0·8	0·15
Mako	0·6	0·02	1·3	0·03
Salmon	0·9	0·02	3·6	0·08
Birds	2·3	0·09	1·4	0·05
Black-footed albatross	3·9	0·28	1·9	0·13
Laysan albatross	1·9	0·09	1·2	0·06
Pinnipeds	0·9	0·03	2·2	0·08
California sea lion	0·9	0·03	2·2	0·08

Fig. 4. Coverage (proportion) of mean location estimates from model fitted to Argos/global positioning system and geolocation data by 95% posterior probability intervals from model fitted only to geolocation data for each species group. Plots are histograms representing the number of individual animals with a given coverage.

while black-footed albatrosses had the lowest percentage (25%). Galápagos sharks had complete coverage with respect to latitude, but the percentages of individuals with ≥95% coverage were much lower for the other shark species, especially salmon sharks (mako = 56%, blue = 57%, salmon = 12%). About 42% and 53% of black-footed and Laysan albatrosses had ≥95% latitude coverage, respectively. Only one sea lion had ≥95% of its mean latitudes from the GPS-and-geolocation model within the 95% intervals from the geolocation-only model.

Discussion

The state-space modelling framework developed and presented here is a flexible, statistically robust method for estimating the precision of location data from double-tagged animals. We applied the model to two particular combinations of location data: Argos or GPS and a specific type of geolocation data derived using a light/SST-based algorithm. Assuming precisions for the Argos and GPS data, we were able to successfully estimate the precision of the geolocation data.

Our estimates of errors in light-based longitude geolocations were comparable to previous findings. Estimated SDs of errors in longitude in our study were about $0.5–1°$ for sharks and sea lions and $2–4°$ for albatrosses. Tests of archival tags at known locations have found mean errors in light-based longitudes of $±0.5°$ or less and SDs $<1°$ (Musyl *et al.* 2001; Beck *et al.* 2002; Phillips *et al.* 2004; Shaffer *et al.* 2005; Schaefer & Fuller 2006). Sibert *et al.* (2003) and Sibert *et al.* (2006) used state-space models to estimate measurement errors in light-based longitudes from geolocation tags attached to free-ranging tuna and found almost all error SDs to be $<1°$. Double-tagging

studies of drifter buoys (Nielsen *et al.* 2006) and sharks (Teo *et al.* 2004) found root mean square errors (RMSE) $<1°$ between GPS or Argos longitude estimates and light-based longitude geolocations. Double-tagging studies of albatrosses found slightly higher SDs of errors of up to $2°$ (Phillips *et al.* 2004; Shaffer *et al.* 2005). It is important to note that these types of reported errors between Argos/GPS data and geolocations (SD and RMSE) are not identical to the geolocation error SDs that we report. The former are calculated from the differences between the two data types while the latter represent residual differences between the geolocation data and the locations estimated by the state-space model.

Errors in light-based longitude geolocations were greatest for the two albatross species. The errors were likely greater for the birds than for the other species because of the birds' faster average travel speed and the number of east–west movements. Light-based longitude geolocations assume that the animal does not move during or between pairs of solar events (sunrise and sunset; Hill 1994). Larger movements between solar events result in less precise estimates of longitude. East-west movements in particular result in apparently earlier or later sunrise and sunset. Longitude geolocation errors were greater for black-footed albatrosses than for Laysan albatrosses, probably because black-footed albatrosses were more active at sunrise and sunset.

Our estimates of longitude error are in units of degrees. Because the distance per degree of longitude decreases with increasing latitude, our longitude error estimates are not necessarily appropriate for latitudes not covered by our data. For example, if geolocation errors were a constant distance, then one would expect larger longitude errors at higher latitudes when expressed in degrees. We only observed this for salmon

sharks at the very highest latitudes, but nevertheless caution should be used when extrapolating our estimated longitude errors to other latitudes.

Our estimates of errors in SST-based latitude geolocations were also comparable to previous findings. We estimated SDs of errors in latitude of about 1–2° for all species except salmon sharks whose estimated error was 4°. Double-tagging studies of a drifter buoy (Nielsen *et al.* 2006) and sharks (Teo *et al.* 2004) have found RMSEs of about 1–1.5° between GPS/Argos latitude estimates and SST-based latitude geolocations. Teo *et al.* (2004) found smaller errors for salmon sharks because most of the data in their study came from lower latitudes (< 50°N; Fig. 2). Shaffer *et al.* (2005) found SDs of errors between Argos latitude estimates and SST-based latitude geolocations in the range of 1–4° in their double-tagging study of albatrosses. We found greater estimated latitude errors for black-footed albatross than for Laysan albatross. Black-footed albatross tend to travel to areas with warmer water (Kappes *et al.* 2010), thus, the differences between the water and air temperature might not have been as great. Smaller air–water temperature differentials are problematic for SST-based latitude geolocation and might have resulted in greater errors. The latitude geolocation data in our study were derived using the same basic algorithm that was used by Teo *et al.* (2004) and Shaffer *et al.* (2005).

When we fit the state-space model only to the geolocation data, the coverage of the mean location estimates from the Argos/GPS-and-geolocation model by the 95% intervals of posterior probability was decent with respect to longitude (about 70% of individuals had ≥95% coverage) but lower with respect to latitude (about 40% of individuals). One cause of low coverage was variability in errors among individual tracks. The group-specific error estimates used in fitting the geolocation-only model were either underestimates or overestimates of the error in a given individual track resulting in either over-fitting or under-fitting, respectively, and poorer coverage. The lowest coverage occurred when geolocation errors were largest and most variable among individuals (black-footed albatross longitude and salmon shark latitude).

A second cause of low coverage was violations of our assumption of random, independent, normally distributed geolocation errors, specifically bias and autocorrelation. The results that coverage was poorer for latitude than for longitude and that bias and autocorrelation were also worse for latitude geolocations support this conclusion. Series of systematically biased errors tended to pull the estimated path away from the true path over time resulting in autocorrelated residuals. Further autocorrelation was induced by the geolocation algorithm itself because each latitude geolocation was partially a function of previous latitudes (Teo *et al.* 2004). The posterior probability intervals were not wide enough to account for this bias and autocorrelation.

There are several likely reasons why the latitude geolocations were sometimes biased in a specific direction. Latitude geolocations for salmon sharks and sea lions exhibited a southward bias. One problem for geolocation with these species was their use of areas with low SST gradients, which was challeng-

ing for the geolocation algorithm. The latitudinal SST gradient was low and not necessarily monotonic at the northern end of the salmon shark range (Teo *et al.* 2004; Ruckert 2007). The geographic area used by the sea lions was small, particularly in relation to the spatial resolution of the SST data. Furthermore, as the geolocation algorithm did not produce estimates over land, there was a greater tendency for southward errors than northward errors in the northern Gulf of Alaska and Southern California Bight. There are inherent limitations to the geolocation algorithm used when tracks are short, the area covered is small and the SST gradient is low.

We could have estimated directional biases in the geolocation data within the state-space framework (Sibert *et al.* 2003), which would have increased the estimated precision of the geolocations. However, the magnitude and direction of bias were variable among individuals within species. Because of this variability, we chose not to account for bias in geolocations for individual tracks, but rather allowed any bias to artificially inflate the estimated random error in the geolocations. Thus, our estimates of geolocation error SDs are larger but also more conservative when applied to other geolocation tracks for these species in these geographic areas. Ideally, bias would be modelled as a function of explanatory covariates such as latitude.

The error estimates that we have presented for light-based longitude and SST-based latitude geolocations (Table 3) can subsequently be used when fitting our state-space model to similar geolocation tracks for which independent information on measurement error is not available. Incorporating these measurement errors in the fitting of the model will result in more appropriate estimates of uncertainty for modelled locations. This uncertainty should then be accounted for in subsequent spatial analyses (Block *et al.* 2011). It is important to recognize that for any one individual track, the overall group-specific errors will likely be lower or higher than the error in the geolocations for that track. Thus, using these group-specific errors will result in over- or under-fitting.

Our modelling study highlighted several aspects of the framework presented here that should be further studied and developed in the future. One improvement would be more appropriate error distributions for the telemetry data as tag technology has evolved rapidly. Several recent studies have examined the accuracy and precision of Argos data using GPS data for reference (Kuhn *et al.* 2009; Tremblay *et al.* 2009; Costa *et al.* 2010; Patterson *et al.* 2010), and an analysis of those results to update Argos location class-specific error distributions would be useful. Information about the distribution of errors in Fastloc GPS data is also highly desirable. There is a large scope for improving the error distributions that we used for light- and SST-based geolocations. The observation model could be extended to allow for serial dependence in geolocations, and this extension would possibly improve the coverage of true locations by the posterior probability intervals of a model fitted to these data. Ideally, the model would be fitted to the raw light and SST data and error distributions would be derived for those data. Lam *et al.* (2010) have developed a state-space model that can be fitted to such data.

A few aspects of our process model could also be developed further. Our model assumed a regular time step with linear movement during each step. Continuous-time state-space models allow for variable lengths of time steps defined by the data themselves (Johnson *et al.* 2008; Gurarie *et al.* 2009; Patterson *et al.* 2010). A continuous-time framework would potentially allow for a more realistic model of animal movement, but may also be challenging to implement in the context of multiple data types and the estimation of observation error parameters. Constraints on movement speed and locations on land could be imposed through prior probability distributions to improve the realism of the posterior probability distributions of tracks when the model is fitted only to geolocation data.

Finally, we fit our model to each individual's data separately, estimating separate parameters for each individual. A hierarchical state-space framework would allow the model to be fitted to multiple individuals simultaneously while estimating distributions of parameters across individuals (Jonsen *et al.* 2006). Such distributions could serve as prior probability distributions for error parameters when fitting the model to novel tracks, potentially eliminating the need to use fixed point estimates.

The state-space framework presented here is a robust statistical approach to analysing location data from double-tagging experiments. This state-space framework has advantages over simple data comparisons because it acknowledges errors in all data, not just the less precise data, and it can accommodate a range of data types with different temporal resolutions. State-space models can be fitted to as many location data types as are available. Furthermore, because the state-space model incorporates an underlying model of animal movement, one can make appropriate inferences about true animal locations and movement while simultaneously estimating measurement errors.

Acknowledgements

References

Beck, C.A., McMillan, J.I. & Bowen, W.D. (2002) An algorithm to improve geolocation positions using sea surface temperature and diving depth. *Marine Mammal Science*, **18**, 940–951.

Block, B.A., Dewar, H., Blackwell, S.B., Williams, T.D., Prince, E.D., Farwell, C.J., Boustany, A., Teo, S.L.H., Seitz, A., Walli, A. & Fudge, D. (2001) Migratory movements, depth preferences, and thermal biology of Atlantic bluefin tuna. *Science*, **293**, 1310–1314.

Block, B.A., Jonsen, I.D., Jorgensen, S.J., Winship, A.J., Shaffer, S.A., Bograd, S.J., Hazen, E.L., Foley, D.G., Breed, G.A., Harrison, A.-L., Ganong, J.E., Swithenbank, A., Castleton, M., Dewar, H., Mate, B.R., Shillinger, G.L., Schaefer, K.M., Benson, S.R., Weise, M.J., Henry, R.W. & Costa, D.P. (2011) Tracking apex marine predator movements in a dynamic ocean. *Nature*, **475**, 86–90.

Buckland, S.T., Newman, K.B., Thomas, L. & Koesters, N.B. (2004) State-space models for the dynamics of wild animal populations. *Ecological Modelling*, **171**, 157–175.

Codling, E.A., Plank, M.J. & Benhamou, S. (2008) Random walk models in biology. *Journal of the Royal Society Interface*, **5**, 813–834.

Costa, D.P., Robinson, P.W., Arnould, J.P.Y., Harrison, A.-L., Simmons, S.E., Hassrick, J.L., Hoskins, A.J., Kirkman, S.P., Oosthuizen, H., Villegas-Amtmann, S. & Crocker, D.E. (2010) Accuracy of ARGOS locations of pinnipeds at-sea estimated using Fastloc GPS. *PLoS One*, **5**, e8677.

DeLong, R.L., Stewart, B.S. & Hill, R.D. (1992) Documenting migrations of northern elephant seals using day length. *Marine Mammal Science*, **8**, 155–159.

Durbin, J. & Koopman, S.J. (2001) *Time Series Analysis by State Space Methods*. Oxford Statistical Science Series. Oxford University Press, Oxford, UK.

Ekstrom, P.A. (2004) An advance in geolocation by light. *Memoirs of the National Institute of Polar Research Special Issue*, **58**, 210–226.

Ekstrom, P. (2007) Error measures for template-fit geolocation based on light. *Deep-Sea Research II*, **54**, 392–403.

Gelman, A. & Rubin, D.B. (1992) Inference from iterative simulation using multiple sequences. *Statistical Science*, **7**, 457–472.

Gelman, A., Carlin, J.B., Stern, H.S. & Rubin, D.B. (2004) *Bayesian Data Analysis*. Texts in Statistical Science. Chapman and Hall/CRC, Boca Raton, Florida.

Gurarie, E., Andrews, R.D. & Laidre, K.L. (2009) A novel method for identifying behavioural changes in animal movement data. *Ecology Letters*, **12**, 395–408.

Hill, R.D. (1994) Theory of geolocation by light levels. *Elephant Seals: Population Ecology, Behavior, and Physiology* (eds B.J. Le Boeuf & R.M. Laws), pp. 227–236. University of California Press, Berkeley, California, USA, 414 pp.

Hooker, S.K., Biuw, M., McConnell, B.J., Miller, P.J.O. & Sparling, C.E. (2007) Bio-logging science: Logging and relaying physical and biological data using animal-attached tags. *Deep-Sea Research II*, **54**, 177–182.

Johnson, D.S., London, J.M., Lea, M.-A. & Durban, J.W. (2008) Continuous-time correlated random walk model for animal telemetry data. *Ecology*, **89**, 1208–1215.

Jonsen, I.D., Flemming, J.M. & Myers, R.A. (2005) Robust state-space modeling of animal movement data. *Ecology*, **86**, 2874–2880.

Jonsen, I.D., Myers, R.A. & James, M.C. (2006) Robust hierarchical state-space models reveal diel variation in travel rates of migrating leatherback turtles. *Journal of Animal Ecology*, **75**, 1046–1057.

Kappes, M.A., Shaffer, S.A., Tremblay, Y., Foley, D.G., Palacios, D.M., Robinson, P.W., Bograd, S.J. & Costa, D.P. (2010) Hawaiian albatrosses track interannual variability of marine habitats in the North Pacific. *Progress in Oceanography*, **86**, 246–260.

Kooyman, G.L. (2004) Genesis and evolution of bio-logging devices: 1963–2002. *Memoirs of the National Institute of Polar Research Special Issue*, **58**, 15–22.

Kuhn, C.E., Johnson, D.S., Ream, R.R. & Gelatt, T.S. (2009) Advances in the tracking of marine species: using GPS locations to evaluate satellite track data and a continuous-time movement model. *Marine Ecology-Progress Series*, **393**, 97–109.

Lam, C.H., Nielsen, A. & Sibert, J.R. (2010) Incorporating sea-surface temperature to the light-based geolocation model TrackIt. *Marine Ecology-Progress Series*, **419**, 71–84.

Lonergan, M., Fedak, M. & McConnell, B. (2009) The effects of interpolation error and location quality on animal track reconstruction. *Marine Mammal Science*, **25**, 275–282.

Lunn, D.J., Thomas, A., Best, N. & Spiegelhalter, D. (2000) WinBUGS – A Bayesian modelling framework: Concepts, structure, and extensibility. *Statistics and Computing*, **10**, 325–337.

McConnell, B.J., Chambers, C. & Fedak, M.A. (1992) Foraging ecology of southern elephant seals in relation to the bathymetry and productivity of the Southern Ocean. *Antarctic Science*, **4**, 393–398.

Metcalfe, J.D. & Arnold, G.P. (1997) Tracking fish with electronic tags. *Nature*, **387**, 665–666.

Morales, J.M., Haydon, D.T., Frair, J., Holsinger, K.E. & Fryxell, J.M. (2004) Extracting more out of relocation data: building movement models as mixtures of random walks. *Ecology*, **85**, 2436–2445.

Musyl, M.K., Brill, R.W., Curran, D.S., Gunn, J.S., Hartog, J.R., Hill, R.D., Welch, D.W., Eveson, J.P., Boggs, C.H. & Brainard, R.E. (2001) Ability of archival tags to provide estimates of geographical position based on light intensity. *Electronic Tagging and Tracking in Marine Fishes* (eds J.R. Sibert & J.L. Nielsen), *Volume 1* . *Reviews: Methods and Technologies in Fish Biology and Fisheries*, pp. 343–367. Kluwer Academic Publishers, Dordrecht, Netherlands, 468 pp.

Nicholls, D.G., Robertson, C.J.R. & Murray, M.D. (2007) Measuring accuracy and precision for CLS:Argos satellite telemetry locations. *Notornis*, **54**, 137–157.

Nielsen, A. & Sibert, J.R. (2007) State-space model for light-based tracking of marine animals. *Canadian Journal of Fisheries and Aquatic Sciences*, **64**, 1055–1068.

Nielsen, A., Bigelow, K.A., Musyl, M.K. & Sibert, J.R. (2006) Improving light based geolocation by including sea surface temperature. *Fisheries Oceanography*, **15**, 314–325.

Patterson, T.A., Thomas, L., Wilcox, C., Ovaskainen, O. & Matthiopoulos, J. (2008) State-space models of individual animal movement. *Trends in Ecology and Evolution*, **23**, 87–94.

Patterson, T.A., McConnell, B.J., Fedak, M.A., Bravington, M.V. & Hindell, M.A. (2010) Using GPS data to evaluate the accuracy of state-space methods for correction of Argos satellite telemetry error. *Ecology*, **91**, 273–285.

Phillips, R.A., Silk, J.R.D., Croxall, J.P., Afanasyev, V. & Briggs, D.R. (2004) Accuracy of geolocation estimates for flying seabirds. *Marine Ecology-Progress Series*, **266**, 265–272.

R Development Core Team (2009) *R: A Language and Environment for Statistical Computing*. R Foundation for Statistical Computing, Vienna, Austria.

Ruckert, M. (2007) *Seasonal Movement and Diving Behavior of the White Shark (Carcharodon carcharias) in the Eastern Pacific Ocean Determined from Pop-Up Archival Tags*. MSc, University Pierre and Marie Curie-Paris VI, Paris.

Schaefer, K.M. & Fuller, D.W. (2006) Comparative performance of current generation geolocating archival tags. *Marine Technology Society Journal*, **40**, 15–28.

Shaffer, S.A., Tremblay, Y., Awkerman, J.A., Henry, R.W., Teo, S.L.H., Anderson, D.J., Croll, D.A., Block, B.A. & Costa, D.P. (2005) Comparison of light- and SST-based geolocation with satellite telemetry in free-ranging albatrosses. *Marine Biology*, **147**, 833–843.

Shaffer, S.A., Tremblay, Y., Weimerskirch, H., Scott, D., Thompson, D.R., Sagar, P.M., Moller, H., Taylor, G.A., Foley, D.G., Block, B.A. & Costa, D.P. (2006) Migratory shearwaters integrate oceanic resources across the Pacific Ocean in an endless summer. *Proceedings of the National Academy of Sciences of the United States of America*, **103**, 12799–12802.

Sibert, J.R., Musyl, M.K. & Brill, R.W. (2003) Horizontal movements of big eye tuna (*Thunnus obesus*) near Hawaii determined by Kalman filter analysis of archival tag data. *Fisheries Oceanography*, **12**, 141–151.

Sibert, J.R., Lutcavage, M.E., Nielsen, A., Brill, R.W. & Wilson, S.G. (2006) Interannual variation in large-scale movement of Atlantic bluefin tuna (*Thunnus thynnus*) determined from pop-up satellite archival tags. *Canadian Journal of Fisheries and Aquatic Sciences*, **63**, 2154–2166.

Sibert, J.R., Nielsen, A., Musyl, M.K., Leroy, B. & Evans, K. (2009) Removing bias in latitude estimated from solar irradiance time series. *Tagging and Tracking of Marine Animals with Electronic Devices* (eds J.L. Nielsen, H. Arrizabalaga, N. Fragoso A. Hobday, M. Lutcavage & J. Sibert), *Volume 9* . *Reviews: Methods and Technologies in Fish Biology and Fisheries*, pp. 311–322. Springer, Dordrecht, Netherlands, 452 pp.

Smith, P. & Goodman, D. (1986) Determining fish movements from an 'archival' tag: precision of geographical positions made from a time-series of swimming temperature and depth. NOAA Technical Memorandum NOAA-TM-NMFS-SWFC- 60, National Marine Fisheries Service.

Teo, S.L.H., Boustany, A., Blackwell, S., Walli, A., Weng, K.C. & Block, B.A. (2004) Validation of geolocation estimates based on light level and sea sur-face temperature from electronic tags. *Marine Ecology-Progress Series*, **283**, 81–98.

Tremblay, Y., Robinson, P.W. & Costa, D.P. (2009) A parsimonious approach to modeling animal movement data. *PLoS One*, **4**, e4711.

Vincent, C., McConnell, B.J., Ridoux, V. & Fedak, M.A. (2002) Assessment of Argos location accuracy from satellite tags deployed on captive grey seals. *Marine Mammal Science*, **18**, 156–166.

Weimerskirch, H., Bonadonna, F., Bailleul, F., Mabille, G., Dell'Omo, G. & Lipp, H.-P. (2002) GPS tracking of foraging albatrosses. *Science*, **295**, 1259.

Weng, K.C., Castilho, P.C., Morrissette, J.M., Landeira-Fernandez, A.M., Holts, D.B., Schallert, R.J., Goldman, K.J. & Block, B.A. (2005) Satellite tagging and cardiac physiology reveal niche expansion in salmon sharks. *Science*, **310**, 104–106.

Wildlife Computers (2005) *WC-GPE: Global Position Estimator Program Suite*. Wildlife Computers, Redmond, Washington, USA.

Supporting Information

Additional Supporting Information may be found in the online version of this article.

Data S1. Supplementary methods including WinBUGS code for Argos/GPS-and-geolocation model, details on tagging and calculation of error estimates.

Table S1. Number of Argos/GPS data ($n_{\mathrm{Argos/GPS}}$), number of geolocation data ($n_{\mathrm{geolocation}}$), model track length (d), estimated SD of errors in longitude ($\widehat{\mathrm{SD}}_{\mathrm{lon}}$) and latitude ($\widehat{\mathrm{SD}}_{\mathrm{lat}}$) geolocations (degrees), SDs of these error estimates ($\sigma_{\widehat{\mathrm{SD}}_{\mathrm{lon}}}$ and $\sigma_{\widehat{\mathrm{SD}}_{\mathrm{lat}}}$), and the proportion of mean estimated longitudes and latitudes from the model fitted to Argos/GPS and geolocation data that fell within the 95% posterior probability interval for the corresponding estimates from the model fitted to only geolocation data (coverage; n = number of locations that were compared between models) for each individual.

Figures S1–S7. State-space model fitted to Argos/GPS and geolocation data for example individual black-footed albatrosses [Supplementary Fig. S1, individuals #5 (a–c), #1 (d–f), #6 (g–i) and #11 (j–l)], Laysan albatrosses [Supplementary Fig. S2, individuals #8 (a–c), #3 (d–f), #13 (g–i) and #10 (j–l)], mako sharks [Supplementary Fig. S3, individuals #1 (a–c), #9 (d–f), #6 (g–i) and #13 (j–l)], blue sharks [Supplementary Fig. S4, individuals #1 (a–c), #2 (d–f), #8 (g–i) and #3 (j–l)], salmon sharks [Supplementary Fig. S5, individuals #28 (a–c), #14 (d–f), #20 (g–i) and #3 (j–l)], Galápagos sharks [Supplementary Fig. S6, individuals #1 (a–c) and #2 (d–f)], and California sea lions [Supplementary Fig. S7, individuals #4 (a–c), #2 (d–f), #5 (g–i) and #6 (j–l)]. Blue and red points represent Argos/GPS location and geolocation estimates, respectively. Blue and red lines represent the mean estimated paths from the state-space model fitted to Argos/GPS and geolocation data simultaneously and only geolocation data, respectively. Dashed lines represent intervals of 95% posterior probability. Light grey lines in panels a, d, g and j represent a sample of estimated paths (n = 100) from the posterior probability distribution of the model fitted to only geolocation data. Triangles indicate known deployment and inverted triangles indicate known recapture locations. Dark grey represents land. Note that some outlying Argos data are outside of the plot boundaries and are not shown.

Figures S8–S11. Prior and posterior probability distributions for SD of errors in longitude ($\mathrm{SD}_{\mathrm{lon}}$) for all individuals. Red lines indicate

means on logscale back-transformed. Much of the prior density was near zero, however, there was non-zero prior density across the full range of the *x*-axis and beyond its upper limit although it is not visible on the plot.

Figures S12–S15. Prior and posterior probability distributions for SD of errors in latitude (SD$_{lat}$) for all individuals. Red lines indicate means on logscale back-transformed. Much of the prior density was near zero, however, there was non-zero prior density across the full

range of the *x*-axis and beyond its upper limit although it is not visible on the plot.

As a service to our authors and readers, this journal provides supporting information supplied by the authors. Such materials may be re-organized for online delivery, but are not copy-edited or typeset. Technical support issues arising from supporting information (other than missing files) should be addressed to the authors.